

Ion trajectories calculation for negatively biased needle cathode in volume discharge plasma

A G Remnev^{1,3,*}, K Uemura¹, A V Kozyrev² and V V Lopatin³

¹ITAC Ltd., Shinmaywa 1-1, Takarazuka 665-0052, Japan

²National Research Tomsk State University, Lenin Avenue 36, Tomsk, 634050, Russia

³Institute of High Technology Physics, Lenin Avenue 2a, Tomsk, 634050, Russia

E-mail: remnev.a@shinmaywa.co.jp,

Abstract. Ion trajectories were simulated for the case of multi-needle negatively biased electrode immersed into the volume type plasma. The model was simplified to the 2d case with planar plasma boundary. The electrical field distribution was calculated with the FEA method. Resulting piece wise function was then used to predict ion trajectories emitted from the plasma sheath boundary. Series of the ion trajectories were simulated for different plasma and accelerating gap parameters using single particle analysis. Distribution of the ion current density along the needle surface and angles of the ion incidence were obtained from the simulation. Experimental and theoretical etching profiles are consistent.

1. Introduction

Ion sputtering is widely used for solving numerous technological problems. One of the most important application is sputter deposition, where the incoming energetic ions are producing the flow of targets material atoms that are consequently deposited on the substrates surface [1]. It is commonly used in the magnetron, ion beam and other sputtering systems. Another very important application for ion sputtering of materials is sputter etching, where the target itself is being processed by the ion flow in order to modify surface properties of the target [1].

Previously we have reported a method in which the ion-plasma sputtering (IPS) was used for sharpening of medical needles by means of sputter etching [2]. The needles were orderly placed in two-dimensional array and underwent bias ion sputtering in the plasma of hot filament hollow cathode plasma generator. Argon was used as the plasma forming gas. Addition of active gas allowed for smoother surface and sharper cutting edges of the resulting needles [3].

Besides the sharpening, an unexpected distinctive non-linear needle shape was observed as the result of IPS treatment [2]. In order to understand the mechanism of such shape modification, the ion flow distribution on the needle surface can be simulated.

There are numerous studies devoted to ion flow simulation for various geometries and plasma properties. The mainstream method is particle-in-cell (PIC) method [4, 5]. It is often used for plasma simulations and can be applied for wide range of the problems. However utilization of existing modeling codes can be time and resource consuming. In the present study we investigate a simplified approach for particular case of multi-needle electrode in plasma, which can give some of the sputtering process characteristics without high computational load and within shorter code



development period. The method includes FEM field calculation, Newton's equations solving and TRIM calculation for sputtering rate angular dependence.

2. Simulation

Mathematically the IPS process can be described with the motion equations for the ions starting from the plasma boundary with near zero velocity and arriving at the needle surface with certain flux density and angle. Ion flux density and angle of incidence at the impact site defines the local sputter rate, which can be interpolated for the whole surface of the target needle by cumulating the local values. To calculate the ions trajectories, one needs to know electric field distribution $E(x,y,z)$ which in this case cannot be calculated directly, so the numerical FEA approach was selected to simulate the distribution. The model was simplified to 2d case and needles were substituted with thin rods in order to reduce the computational load.

The plasma boundary from which the ions are extracted is generally of complex shape, dictated by the plasma density and the voltage drop across the plasma sheath.

However we can consider two particular cases: [i] the plasma density is relatively high and the voltage is relatively low, so the plasma leaks into the gaps between the rods; [ii] the plasma density is relatively low and the voltage is relatively high, so the double layer is getting large and the ion emission surface become nearly planar. In the present study, only the second case was investigated. Space charge in the plasma sheath was neglected. The width for the planar plasma sheath can be estimated from the Child-Langmuir equation.

2.1. Electric field distribution

Electric field distribution across the acceleration gap was evaluated with FEA software Maxwell 2d. Input data for the analysis consists of following: needle electrode geometry, acceleration gap (i.e. distance from the plasma boundary to the needles tips) and applied voltage. The values were taken from the range of actual parameters used during the IPS (see Table 1).

Table 1. Input parameters

| Parameters | Values |
|---------------------------------|------------|
| Bias voltage U , V | -400 |
| Pitch between rods p , mm | 5 |
| Length L , mm | 10 |
| Rod diameter d , mm | 0.2 |
| Acceleration gap width D , mm | 2, 4, 6, 8 |

The acceleration gap width D was varied from 2mm to 8mm; different values for D represent different plasma densities, according to Child-Langmuir equation. The working pressure during the actual process is $P=0.4\text{Pa}$, so the acceleration gap was considered collisionless. Domain of study dimensions were $70\text{mm}\times 42\text{mm}$. Resulting electrical field distribution is shown on figure 1 for the case of $D=4\text{mm}$.

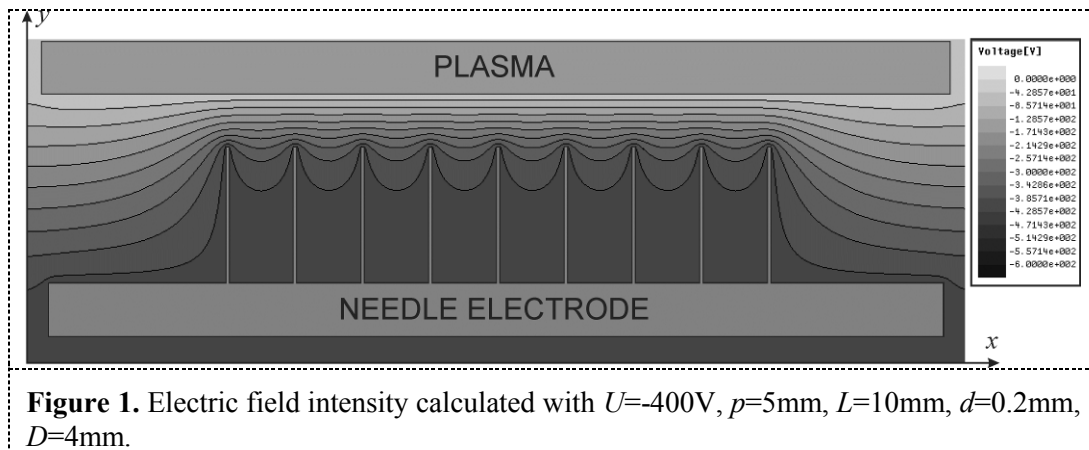


Figure 1. Electric field intensity calculated with $U=-400\text{V}$, $p=5\text{mm}$, $L=10\text{mm}$, $d=0.2\text{mm}$, $D=4\text{mm}$.

2.2. Ion trajectories

In order to calculate the probe ion trajectory the domain of study was divided into rectangular shape cells with the nodes $[X[i], Y[j]]$. Then the electric field distribution obtained with the FEA (see figure 1) was mapped on the rectangular mesh. The electric field within one cell is assumed to be an average of the nodular values.

Having two matrixes of coordinates $[X[i], Y[j]]$ and electric field $[E_x[i,j], E_y[i,j]]$ components one can analytically calculate whole trajectory of an ion injected from the plasma boundary into the acceleration gap. Once the ion leaves the boundary towards the needle cathode it will unavoidably enter a cell with known constant electric field. Then within the cell the motion equations can be analytically solved:

$$\begin{aligned} X[i \pm 1] &= \frac{E_x[i, j] \cdot e}{2 \cdot m} \cdot t^2 + v_x \cdot t + x \\ Y[j \pm 1] &= \frac{E_y[i, j] \cdot e}{2 \cdot m} \cdot t^2 + v_y \cdot t + y, \end{aligned} \quad (1)$$

where m – ion mass, e – electron charge, v_x, v_y – ion velocity components which it had on point of entering the current cell, $X[i \pm 1], Y[j \pm 1]$ coordinates of the cells borders, where the probe ion leaves the current cell and enter the next cell. For the next cell similar equations (1) are solved with different input parameters. The procedure repeats until the ion reaches the needle electrode or leaves the domain of study. By selecting different injection points for the probe ions, a series of trajectories can be obtained and consequently ions individual incidence angle and local linear current density at the rods surface can be derived.

2.3. Ion current and incidence angle

As can be understood from the figure 1 the ion trajectories will have the same pattern for all the needles except the first and the last needle in the array. Thus, the ion current density distribution was simulated for the needle inside the array in order to rule out the edge effect. Small step size of $7.5\mu\text{m}$ between the probe ion injection points was used in order to achieve sufficient accuracy. The distance from the plasma boundary to the needle tips has been varied (see figure 2). Resulting y -coordinate of the ions impact and angles of incidence θ were plotted (see figure 3). The distributions are calculated along the vertical coordinate on the selected rod – y_r , with $y_r=24\text{mm}$ coordinate indicating the upper end of the rod and $y_r=14\text{mm}$ – the bottom end.

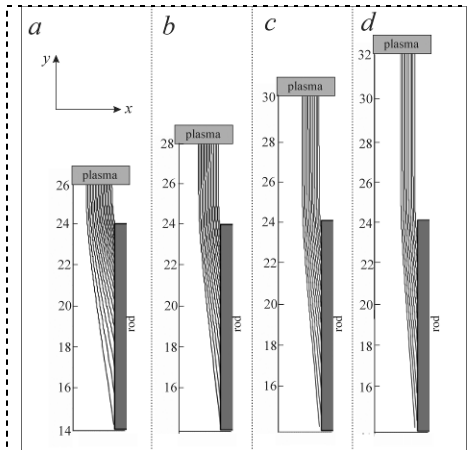


Figure 2. Ion trajectories series for $U=-400V$ and $D=2mm$ (a), $D=4mm$ (b), $D=6mm$ (c), $D=8mm$ (d).

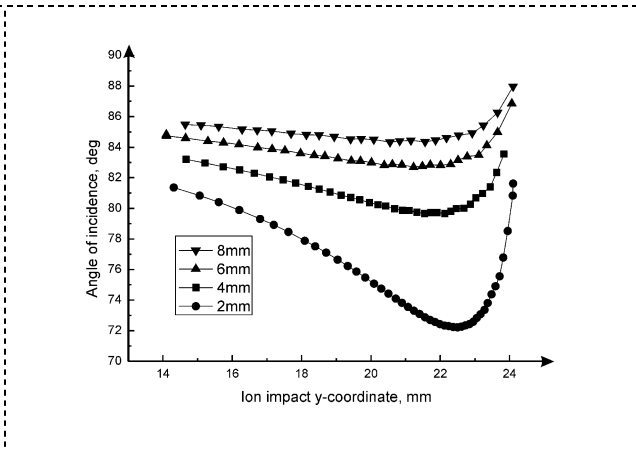


Figure 3. Ion angle of incidence distribution.

2.4. Sputter rate

Sputtering rate distribution along the rod can be evaluated using combination of ion current density and sputtering yield distributions. The latter is angle dependent value, therefore $Y(\theta)$ for $0.4KeV Ar^+$ striking Fe target was calculated with SRIM software at several angles within 70 - 90 degree range (see figure 4) and then interpolated with 2 degree polynomial function as:

$$Y(\theta) = -4.14 + 0.18 \cdot \theta - 0.0014 \cdot \theta^2 \quad (2)$$

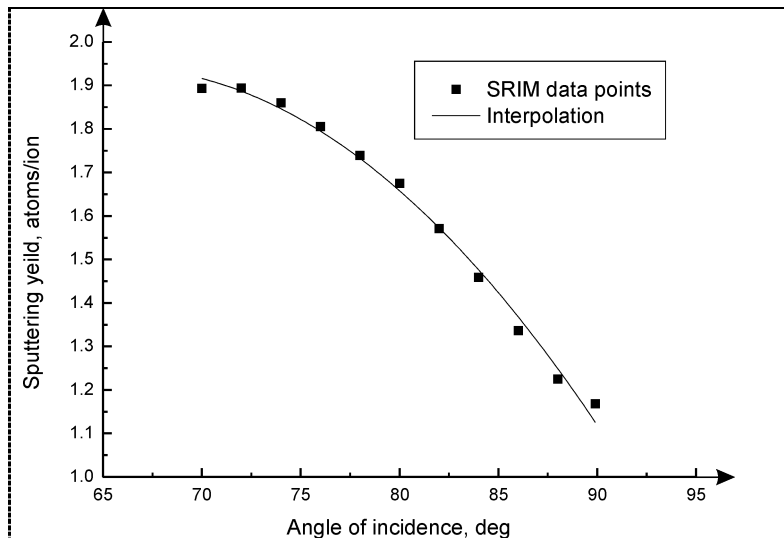


Figure 4. Sputtering yield as function of incidence angle

The yield distribution $Y(y_r)$ along the rod can be found as:

$$Y(y_r) = Y(\theta(y_r)), \quad (3)$$

while the angle of incidence can be found as:

$$\theta(y_r) = arctg(v_{xf}(y_r)/v_{yf}(y_r)), \quad (4)$$

where $v_x(y_r)$ and $v_y(y_r)$ are final velocity components at the ion impact point.

Relative linear current density $j(y_r)$ was interpolated from the density of the calculated trajectory lines on the rods surface; the value depends on the step size between the emitted probe ions. Resulting dimensionless sputtering rate:

$$S(y_r) = Y(y_r) \cdot j(y_r) \quad (5)$$

Simulated $S(y_r)$ is given on the figure 5.

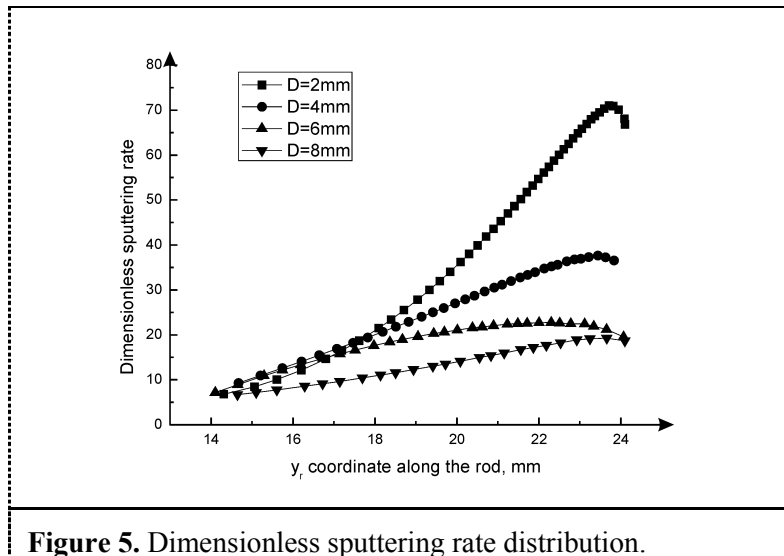


Figure 5. Dimensionless sputtering rate distribution.

3. Experiment

Model experiment with thin rods was carried out in order to validate the simulation approach. The rods were set in 2d array with pitch of 5mm. The plasma was generated with hollow cathode hot filament plasma source; negative 400V bias was applied to the array of the rods. The acceleration gap thickness D was visually evaluated to be about 4mm. The SEM images of the rod before and after the process are compared on the figure 6.

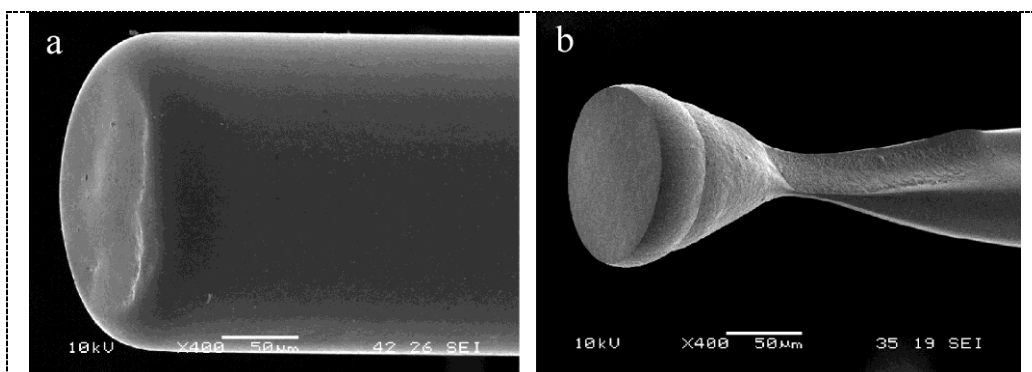


Figure 6. Scanning electron micrographs of stainless steel rods before (a) and after (b) sputtering, with $U=-400$ V and $D\approx 4$ mm, $p=5$ mm, $L=10$ mm and $d=0.2$ mm.

4. Discussion

Calculated sputtering rate distribution (see figure 5) in case of 2mm, 4mm and 6mm D has prominent peak near the upper end of the rod in the similar manner to the experimentally etched profile. Having the results of the simulation one can say that the etched profile is formed due to the [i] angular sputtering yield dependence, which is monotonously decreasing with the incidence angles in the range from 70 to 90 degree (see figure 4), [ii] incidence angle distribution along the rods vertical axis which has a peak near the end of the rod (see figure 3) and [iii] ion current density distribution along the rods vertical axis. Thus, the simulation clarified the reasons of the non-linear shape formation obtained in the experimental IPS on the rods and needles. This computational approach can also give a good opportunity for understanding in which way the process needs to be adjusted when specific shape is required.

5. Conclusion

In the present study simplified 2d simulation method for the bias IPS process was suggested and carried out using combination of FEA and analytical motion equations solving. The results of the simulation are showing the same trend as the experimental results, thus this rather simple computational method can be used for estimation of the ion flow and sputtering distribution. Further model refining and experimental data accumulation can give a deeper understanding of the ion flow driven shape modification of sputtered needles as well as more numerical results. The case of non-planar plasma boundary is good candidate for following study.

References

- [1] Behrisch R and Eckstein W 2007 *Sputtering by Particle Bombardment* (New York: Springer).
- [2] Remnev A G, Shalnov K V, Uemura K and Nagato K 2012 *ISPlasma: Proceedings of the 4th International Symposium on Advanced Science and its Applications for Nitrides and Nanomaterials* (Chubu University, Aichi, Japan) 79.
- [3] Alghuraira O, Remnev A G, Nagato K, Ikeshima S, Yasunoria O, Uemura K and Nakao M 2013 *Procedia CIRP* **5** 53-56.
- [4] Ledvina S A, Ma Y J and Kallio E 2008 *Space Science Reviews* 139.
- [5] Birdsall C K 1991 *IEEE Transactions on Plasma Science* 19 65-85.